

# Development and Investigation of Polyaniline Micro/nanocomposites that Possess Moderate Conductivity, Dielectric and Magnetic Properties

By Sook-Wai PHANG and Noriyuki KURAMOTO\*

As a nano-material possessing moderate conductivity, magnetic and dielectric property, novel hexanoic acid doped polyaniline (PAni/HA) micro/nanocomposites containing TiO<sub>2</sub> and Fe<sub>3</sub>O<sub>4</sub> were prepared by template free method under various polymerization conditions. FT/IR spectra of PAni/HA/TiO<sub>2</sub> and PAni/HA/TiO<sub>2</sub>/Fe<sub>3</sub>O<sub>4</sub> indicated the peaks are derived from PAni/HA. The X-ray diffraction patterns of PAni/HA/TiO<sub>2</sub> and PAni/HA/TiO<sub>2</sub>/Fe<sub>3</sub>O<sub>4</sub> clearly showed the existence of both TiO<sub>2</sub> and Fe<sub>3</sub>O<sub>4</sub>. Nanorods/tubes shown in the SEM images indicated that PAni/HA, PAni/HA/TiO<sub>2</sub> and PAni/HA/TiO<sub>2</sub>/Fe<sub>3</sub>O<sub>4</sub> micro/nanocomposites exhibited polymerization through elongation. The diameters of PAni/HA nanorods/tubes increased from 150–180 nm to 180–200 nm (PAni/HA/TiO<sub>2</sub> and PAni/HA/TiO<sub>2</sub>/Fe<sub>3</sub>O<sub>4</sub>) after addition of Fe<sub>3</sub>O<sub>4</sub> and TiO<sub>2</sub>. PAni/HA, PAni/HA/TiO<sub>2</sub> and PAni/HA/TiO<sub>2</sub>/Fe<sub>3</sub>O<sub>4</sub> synthesized at 0 °C resulted large amount of nanorods/tubes compared with those synthesized at 25 °C. PAni/HA polymerized at low temperature exhibited higher conductivity ( $1.0 \times 10^{-3}$  S/cm) compared with PAni/HA polymerized at higher temperature ( $7.0 \times 10^{-4}$  S/cm). The conductivities of the PAni/HA/TiO<sub>2</sub> and PAni/HA/TiO<sub>2</sub>/Fe<sub>3</sub>O<sub>4</sub> were relatively low ( $3.3\text{--}4.2 \times 10^{-4}$  S/cm) after addition of TiO<sub>2</sub> and Fe<sub>3</sub>O<sub>4</sub>. PAni/HA/TiO<sub>2</sub>/Fe<sub>3</sub>O<sub>4</sub> micro/nanocomposites synthesized at 0 °C exhibited higher magnetization ( $M_s = 7.7$  emu/g) compare with micro/nanocomposites that synthesized at 25 °C ( $M_s = 4.7$  emu/g). TGA characterizations of the micro/nanocomposites were also being discussed in this paper.

KEY WORDS: Polyaniline / Micro/nanocomposites / Conductivity / Magnetization / Dielectric Constant /

Recently, micro/nanotubes or micro/nanowires have attracted considerable attention because of their unique properties and promising potential applications in nanodevices.<sup>1–4</sup> Conducting polymer as molecular wires (micro/nanowires) is an excellent choice because of their long  $\pi$ -conjugation length as well as their high metal conductivity ( $10^3\text{--}10^5$  S/cm).<sup>5</sup> Among conducting polymers, polyaniline (PAni) and its analogues as micro/nanowires have been studied most extensively because their good environmental stability in both doped and undoped forms, low cost and ease of preparation, excellent physical and chemical properties, unique doping mechanism and its ease of protonic acid doping in the emeraldine form.<sup>6,7</sup>

A series of up to date methods have been reported for synthesizing micro-/nanotubes of conducting polymers, such as template synthesis, electrospinning, chiral nematic reaction and molecular beam deposition.<sup>8,9</sup> However, template free method is an excellent route to synthesize the micro/nanotubes of conducting polymers because the micelle consists of dopant or dopant/aniline salt could act as a “soft template” in the formation of the nanostructured PAni by omitting the using of “hard template” (e.g. Al<sub>2</sub>O<sub>3</sub> or polycarbonate). This method is easy and cheap due to the controllable diameter and length of the micro/nanotubes by alternating the synthesis parameters such as the types of dopants, polymerization temperature used and etc.<sup>10–12</sup>

Electromagnetic radiation is one of the byproduct of rapid

development in space technology, navigation, telecommunication, aircraft technology and rapid proliferation of electronic devices. These rapid development and proliferation have generated pollution in the form of electromagnetic interference (EMI).<sup>13</sup> Generally, the active components commonly used in the traditional microwave absorbing and shielding material are dielectric and magnetic materials. Extensive study has been carried out to develop microwave-absorption materials and shielding materials with high efficiency. High conductivity, magnetic permeability and dielectric permittivity of the materials contribute to high EMI shielding efficiency (SE) and good microwave absorbing property.<sup>14</sup> Thus, it is really a challenge to tailoring the synthesis parameters or additives used in order to synthesize a new series of PAni micro/nanowires possessing moderate conductivity, magnetic and dielectric properties.

The focus of this work is to develop and characterize a PAni micro/nanomaterial exhibits moderate conductivity, magnetic and dielectric properties. Recently, PAni/naphthalene sulphonic acid/Fe<sub>3</sub>O<sub>4</sub> nanocomposite was reported to exhibit good magnetic properties,<sup>15</sup> whereby PAni/HCl/TiO<sub>2</sub> nanocomposite was also reported to show a large dielectric constant.<sup>16</sup> Hence, PAni/Dopant/TiO<sub>2</sub>/Fe<sub>3</sub>O<sub>4</sub> nanocomposite should be an excellent microwave absorbing and shielding material because TiO<sub>2</sub> and Fe<sub>3</sub>O<sub>4</sub> used in this study are the dielectric and magnetic filler that could enhance the dielectric and

Graduate School of Human Sensing and Functional Sensor Engineering, Graduate School of Science and Engineering, Yamagata University, 4-3-16 Jonan, Yonezawa Yamagata 992-8510, Japan

\*To whom correspondence should be addressed (Tel: +81-23-826-3051, Fax: +81-23-826-3051, E-mail: kuramoto@yz.yamagata-u.ac.jp).

magnetic property of the PANi. Besides that, hexanoic acid used is the dopant which could improve the conductivity of the PANi. However, the preparation and characterization of such composite have not reported yet.

In this study, as a nano-material possessing moderate conductivity, magnetic property and dielectric property, novel hexanoic acid doped PANi (PANi/HA) micro/nanocomposites containing TiO<sub>2</sub> and Fe<sub>3</sub>O<sub>4</sub> (PANi/HA/TiO<sub>2</sub> and PANi/HA/TiO<sub>2</sub>/Fe<sub>3</sub>O<sub>4</sub>) were prepared by template free method using ammonium persulfate, APS as an oxidizing agent under various polymerization conditions. At the starting point of this research, weak acid such as hexanoic acid (HA) was chosen as a dopant because the acidity of the dopant will strongly effect the magnetization of the composites. Besides that, Fe<sub>3</sub>O<sub>4</sub> microparticles was used instead of Fe<sub>3</sub>O<sub>4</sub> nanoparticles because the spin magnet of Fe<sub>3</sub>O<sub>4</sub> nanoparticles could not well align but just keep vibrating. These phenomena finally reduce the magnetization of Fe<sub>3</sub>O<sub>4</sub> nanoparticles ( $M_s = 65 \text{ emu/g}$ )<sup>8</sup> compared with Fe<sub>3</sub>O<sub>4</sub> microparticles ( $M_s = 87 \text{ emu/g}$ ) that used in this study. PANi micro/nanocomposites were then characterized by FT/IR, X-ray diffraction (XRD) and thermogravimetric (TGA) analysis. Morphology studies of the micro/nanocomposites were investigated *via* SEM. Besides that, conductivity, magnetic and dielectric behaviors of the micro/nanocomposites were being studied in this communication.

## EXPERIMENTAL

Aniline (Ani), n-hexanoic acid (HA) and ammonium peroxydisulfate (APS) used in this study were purchased from Kanto Chemicals. Tri-iron tetra-oxide microparticles (Fe<sub>3</sub>O<sub>4</sub>) with particle size of 1  $\mu\text{m}$  (purity 99%) and TiO<sub>2</sub> nanoparticles with particle size of 30 nm were ordered from Soekawa Chemicals and Tayca Corporation respectively. The crystal phase of TiO<sub>2</sub> used this study is in anatase form because it is economical and anatase form of TiO<sub>2</sub> easily dispersed in water based systems or aqueous systems. Water used for polymerization was purified by distillation. Other reagents were used as received without purification unless noted.

In this study, hexanoic acid doped polyaniline (PANi/HA) micro/nanocomposites containing TiO<sub>2</sub> and Fe<sub>3</sub>O<sub>4</sub> (PANi/HA/TiO<sub>2</sub> and PANi/HA/TiO<sub>2</sub>/Fe<sub>3</sub>O<sub>4</sub>) were prepared by template free method using APS as an oxidizing agent under various polymerization conditions.

First, HA ( $1.0 \times 10^{-2} \text{ mol}$ ) and Ani ( $1.0 \times 10^{-2} \text{ mol}$ ) were mixed vigorously in distilled water for 30 min. Then, 0.10 g of TiO<sub>2</sub> (nanoparticles, 30 nm) and 0.10 g of Fe<sub>3</sub>O<sub>4</sub> (microparticles, 1  $\mu\text{m}$ ) were added into the solution under sonication in order to obtain an emulsion of Ani/HA complex containing TiO<sub>2</sub> and Fe<sub>3</sub>O<sub>4</sub>. The emulsion of Ani/HA complex containing TiO<sub>2</sub> and Fe<sub>3</sub>O<sub>4</sub> was mixed vigorously under ultrasonic action for 4 h to disperse TiO<sub>2</sub> and Fe<sub>3</sub>O<sub>4</sub> well into the Ani/HA mixture before polymerization. APS aqueous solution was added dropwise in the mixture at 0 °C within 2 h. The Ani/HA/APS ratio used is 1/1/1. After addition of APS, the mixture was stirred under sonication for 1 h. Polymerization was

continued (undisturbed) for 12 h by maintaining the temperature at 0 °C in the ice bath. The micro/nanocomposites were washed with distilled water and methanol three times, respectively. The nanocomposites were then dried in vacuum for 24 h.

The same polymerization method was repeated for PANi/HA, PANi/HA/TiO<sub>2</sub> and PANi/HA/TiO<sub>2</sub>/Fe<sub>3</sub>O<sub>4</sub> micro/nanocomposite (with and without TiO<sub>2</sub> and Fe<sub>3</sub>O<sub>4</sub>) at room temperature (considered as 25 °C).

The characterizations of the PANi micro/nanocomposites were carried out by FT/IR, XRD, thermogravimetric analysis (TGA) and SEM. The FT/IR measurements in KBr in discus shape were taken by Shimadzu FT/IR (type 8100M) spectrometer in between 400–4000  $\text{cm}^{-1}$ . The X-ray diffraction patterns of the PANi micro/nanocomposite were recorded using RINT2000 Wilder-angle goniometer using Cu K $\alpha$  radiation. Thermograms of the PANis were recorded using Mettler-Toledo 851 thermogravimetric analyzer, in the presence of N<sub>2</sub> atmosphere from room temperature to 600 °C with heating rate of 10 °C/min. Particles sizes and morphology behaviors of the PANi micro/nanocomposite were determined from scanning electron microscope, SEM (JSM-6300F).

Samples used for conductivity measurements were in discus shape form with diameter of 10 mm and thickness of 0.3–0.5 mm. The sample was compressed slowly using a constant load of 100 kg and the whole process took around 5–10 min. Samples obtained with compacted density of  $1.09 \times 10^3 \text{ kg/m}^3$  were tested using a standard four-probe method (model Loresta HP).

The relative dielectric constants ( $\epsilon_r$ ) are obtained from the measurements of capacitance (C) and dissipation factor (D) by a 4192A LF Yokogawa Howlett Packard impedance analyzer in the frequency range of 5 Hz to 13 MHz. Samples used for the measurement were in discus shape that coated with the silver paste. The role of the silver paste is as the electrical contacts during measurement. The permittivity of the material is evaluated by the relation  $C = \epsilon_s A/t$ , in which t is the thickness of the samples and A is the area of the discus shape's surface. The relative dielectric constant,  $\epsilon_r$  is calculated from  $\epsilon_r = \epsilon_s' / \epsilon_0$ .

Magnetization of PANi samples at magnetic field from  $-1.0 \times 10^4 \text{ Oe}$  to  $1.0 \times 10^4 \text{ Oe}$  were measured at room temperature by vibrating sample magnetometer (VSM), model 1660 signal processor.

## RESULTS AND DISCUSSION

The FT/IR spectra of PANi/HA, PANi/HA/TiO<sub>2</sub> and PANi/HA/TiO<sub>2</sub>/Fe<sub>3</sub>O<sub>4</sub> micro/nanocomposites are shown in Figure 1. The peaks at 1572  $\text{cm}^{-1}$  and 1497  $\text{cm}^{-1}$  are representing the quinoid and benzenoid ring, while the peaks at 1300  $\text{cm}^{-1}$  and 1248  $\text{cm}^{-1}$  are indicating the C-N stretching vibration of PANi. The peak at 1148  $\text{cm}^{-1}$  is due to quinoid unit of doped-PANi. The stretching of CH<sub>3</sub> and CH<sub>2</sub> at 2928  $\text{cm}^{-1}$  and 2853  $\text{cm}^{-1}$  as well as the vibration mode of C=O at 1750  $\text{cm}^{-1}$  are corresponding to the HA that used as the dopant

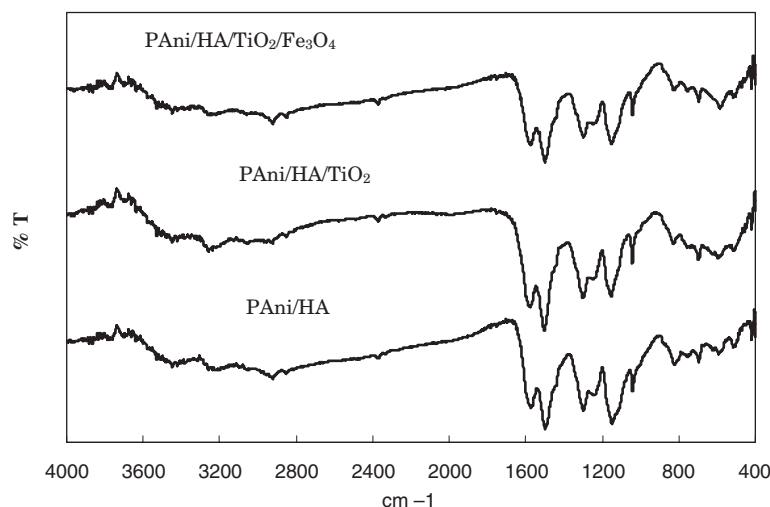


Figure 1. FT/IR spectra of PANi/HA, PANi/HA/TiO<sub>2</sub> and PANi/HA/TiO<sub>2</sub>/Fe<sub>3</sub>O<sub>4</sub> micro/nanocomposites.

in this study.<sup>9</sup> The peaks that mentioned above existed in all PANi/HA, PANi/HA/TiO<sub>2</sub> and PANi/HA/TiO<sub>2</sub>/Fe<sub>3</sub>O<sub>4</sub> micro/nanocomposites that synthesized during this study. For PANi/HA/TiO<sub>2</sub>/Fe<sub>3</sub>O<sub>4</sub> micro/nanocomposite, the band at 598 cm<sup>-1</sup> is attributed to the presence of the Fe<sub>3</sub>O<sub>4</sub>.<sup>17</sup> The incorporation of TiO<sub>2</sub> in the nanocomposites leads to small shift of FT/IR peaks in the nanocomposites.<sup>16</sup>

The X-ray diffraction patterns of the PANi micro/nanocomposite were recorded by Wilder-angle goniometer using Cu K $\alpha$  radiation. Refer to the X-ray diffraction patterns shown in Figure 2, PANi/HA showed amorphous behavior with three major peaks for the characterization of doped-PANi. The peak at  $2\theta = 7.0^\circ$  is ascribed to the periodicity distance between the HA dopant and N atom of PANi on adjacent main chains of PANi/HA. However, the peaks at  $2\theta = 20.3^\circ$  and  $25.0^\circ$  are assigned as the periodicity parallel and perpendicular of the chain direction of the PANi chains.<sup>9</sup> On the other hand, both PANi/HA/TiO<sub>2</sub> & PANi/HA/TiO<sub>2</sub>/Fe<sub>3</sub>O<sub>4</sub> micro/nanocomposites indicated the presence of TiO<sub>2</sub> as predicted by the peaks belong to TiO<sub>2</sub> such as  $2\theta = 25.3^\circ$  and  $48.0^\circ$ .<sup>18,19</sup> In the PANi micro/nanocomposite, the crystal phase of the TiO<sub>2</sub> is not

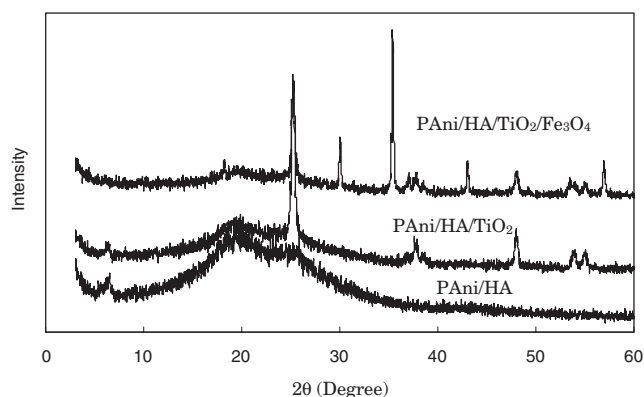


Figure 2. X-Ray diffraction patterns of PANi/HA, PANi/HA/TiO<sub>2</sub> and PANi/HA/TiO<sub>2</sub>/Fe<sub>3</sub>O<sub>4</sub> micro/nanocomposites.

changed because the characteristic peaks of TiO<sub>2</sub> are remained the same even after polymerization as shown by the X-ray diffraction patterns. Furthermore, the existence of Fe<sub>3</sub>O<sub>4</sub> in PANi/HA/TiO<sub>2</sub>/Fe<sub>3</sub>O<sub>4</sub> micro/nanocomposites was also determined by the peaks belong to Fe<sub>3</sub>O<sub>4</sub> such as  $2\theta = 35.4^\circ$ ,  $30.1^\circ$ ,  $18.3^\circ$ ,  $43.1^\circ$  and  $57.0^\circ$ .<sup>20,21</sup>

The thermal stability of PANi micro/nanocomposites were recorded by using thermogravimetric analysis. The thermogram obtained is shown in Figure 3 from room temperature to 600 °C. In TGA profile of PANi micro/nanocomposites, major losses of weight were observed over four temperature periods. Generally, the first decrease of weight loss from room temperature to 100 °C is attributed to the evaporization of water molecules or moistures and also the loss of possible impurities such as remaining monomer. The second stage observed from 100 °C to 230 °C is due to the loss of the HA dopant from PANi chains. The third stage from 230 °C to 350 °C is responsible for the dedoping of HA dopant from backbone of PANi. Finally, the last stage observed from 340 °C onwards is attributed to the complete degradation and structural decomposition of PANi. In the temperature range of 100 °C to 350 °C, the weight loss of PANi/HA/TiO<sub>2</sub> is greater than PANi/HA while PANi/HA/TiO<sub>2</sub>/Fe<sub>3</sub>O<sub>4</sub> is more thermally stable than PANi/HA and PANi/HA/TiO<sub>2</sub>. It can be explained by the fact that a strong interaction exists at interface of TiO<sub>2</sub> and PANi weakens the interactive force of PANi interchains and finally fasten the thermal decomposition of PANi in the composites.<sup>22</sup> However, existence of Fe<sub>3</sub>O<sub>4</sub> in the micro/nanocomposites significantly enhanced the interactive force of PANi chain and also the interaction between PANi with TiO<sub>2</sub>, thus improved the thermal stability of the PANi/HA/TiO<sub>2</sub>/Fe<sub>3</sub>O<sub>4</sub> micro/nanocomposites if compared with micro/nanocomposites without addition of Fe<sub>3</sub>O<sub>4</sub>. The contents of Fe<sub>3</sub>O<sub>4</sub> in PANi/HA/TiO<sub>2</sub>/Fe<sub>3</sub>O<sub>4</sub> micro/nanocomposites synthesized at 0 °C are higher (25%) compared with synthesized at 25 °C (10%) as indicated by the TGA profile below. Although the mass of Fe<sub>3</sub>O<sub>4</sub> adding into the PANi/HA/TiO<sub>2</sub>/Fe<sub>3</sub>O<sub>4</sub> micro/

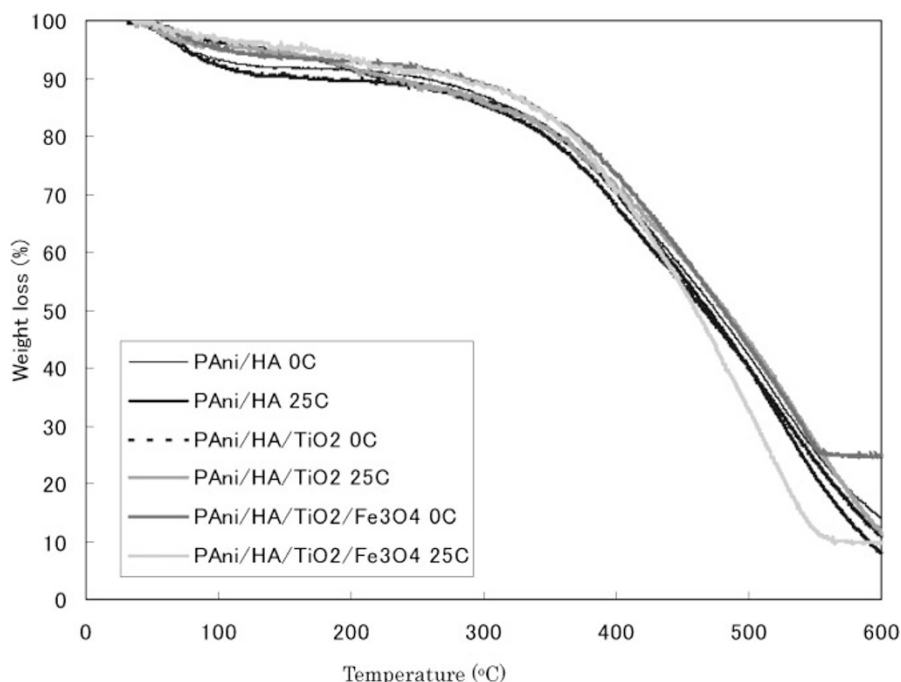


Figure 3. Thermograms of PAni/HA, PAni/HA/TiO<sub>2</sub> and PAni/HA/TiO<sub>2</sub>/Fe<sub>3</sub>O<sub>4</sub> micro/nanocomposites.

nanocomposites synthesized at 0 °C and 25 °C is same (0.1 g), Fe<sub>3</sub>O<sub>4</sub> could easily interact with PAni to form the PAni/HA/TiO<sub>2</sub>/Fe<sub>3</sub>O<sub>4</sub> micro/nanocomposites at low temperature (0 °C) compared with high temperature (25 °C). This fact also can be proved by the magnetization data.

SEM images shown in Figure 4 indicated that Fe<sub>3</sub>O<sub>4</sub> and TiO<sub>2</sub> micro/nanoparticles used in this study are ball-like shapes with diameter of 1 μm and 30 nm, respectively. During template free method, micelle composed of Ani/HA or Ani/HA/TiO<sub>2</sub> salt act as a “soft template” in order to form of the PAni nanotubes/rods (Figure 5). TiO<sub>2</sub> nanoparticles is believed to be existed in the center of the Ani/HA micelle to form the nanorods/tubes. On the other hand, Ani is assigned as the shell due to the hydrophobicity of Ani and HA is acted as the tail of the micelles due to the hydrophilicity of –COOH of HA dopant. Since there is repulsive interactions of the “tail” group (HA group) of the micelle, thus the micelles are exist as a fluid surface and the spherical micelles are expected to form through aggregation process first before the formation of nanorods/tubes (through elongation) or spheres (through accretion) due to the lowest surface energy. Polymerization of these nanocomposites might take place in the micelle/water interface because APS oxidant used is water soluble. The micells become big sphere by accretion or tubes/rods by elongation depend on the synthesis conditions during polymerization process. For example, during template free method, polymerization of Ani/dopant under stirring process might form the PAni spheres, however, polymerization of Ani/dopant under undisturbed state might form the nanorods/tubes.<sup>9</sup>

Nanorods/tubes that shown in the morphology below indicated that PAni/HA, PAni/HA/TiO<sub>2</sub> and PAni/HA/TiO<sub>2</sub>/Fe<sub>3</sub>O<sub>4</sub> micro/nanocomposites exhibited polymerization

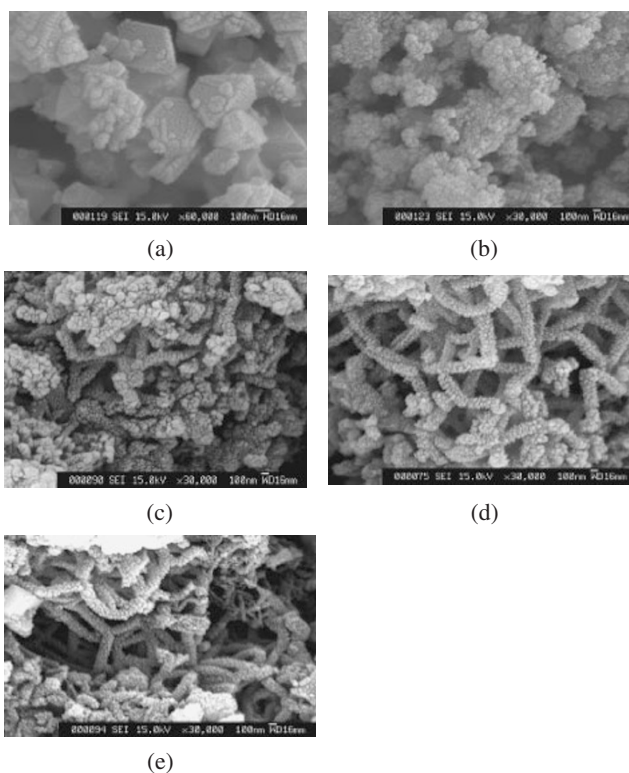
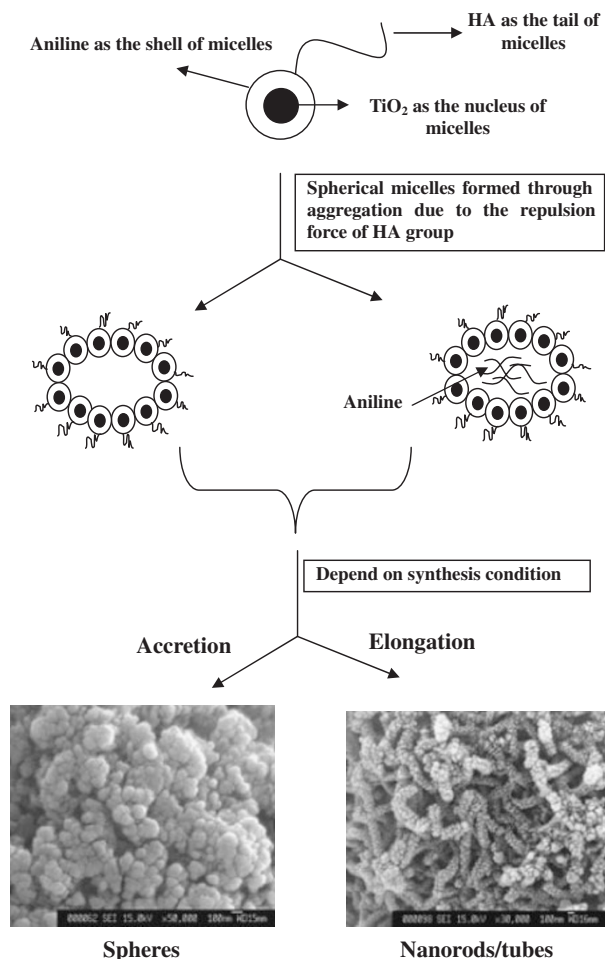


Figure 4. SEM images of (a) Fe<sub>3</sub>O<sub>4</sub> microparticles (60,000x magnification), (b) TiO<sub>2</sub> nanoparticles (30,000x magnification) (c) PAni/HA, 0 °C (30,000x magnification) (d) PAni/HA/TiO<sub>2</sub>, 0 °C micro/nanocomposites (30,000x magnification) and (e) PAni/HA/TiO<sub>2</sub>/Fe<sub>3</sub>O<sub>4</sub>, 0 °C micro/nanocomposite (30,000x magnification).



**Figure 5.** Schematic images for the formation of PANi spheres or PANi nanorods/tubes from the Ani/HA/TiO<sub>2</sub> micelle.

through elongation. As shown in Figure 6, the micelle filled with aniline will form the nanorods while the micelle without aniline will form the nanotubes. The nanorods/tubes obtained in this study are formed by the Ani/HA micelles with TiO<sub>2</sub> as nucleus and Ani/HA micelles without TiO<sub>2</sub> as nucleus. So, the formations of the nanorods/tubes are not just depend on the TiO<sub>2</sub> content in the nanocomposites. The Ani/HA/TiO<sub>2</sub> micelle mechanism that proposed here agreed with the Ani/salicylic acid/TiO<sub>2</sub> micelle mechanism that reported by Zhang *et al.*<sup>11</sup>

Fe<sub>3</sub>O<sub>4</sub> microparticles are physically mixed with the PANi/HA/TiO<sub>2</sub> nanotubes/rods to form the PANi/HA/TiO<sub>2</sub>/Fe<sub>3</sub>O<sub>4</sub> micro/nanocomposites (Figure 7). The diameter of PANi/HA nanorods/tubes increased from 150–180 nm to 180–200 nm (PANi/HA/TiO<sub>2</sub> & PANi/HA/TiO<sub>2</sub>/Fe<sub>3</sub>O<sub>4</sub>) after addition of Fe<sub>3</sub>O<sub>4</sub> and TiO<sub>2</sub>. PANi/HA, PANi/HA/TiO<sub>2</sub> and PANi/HA/TiO<sub>2</sub>/Fe<sub>3</sub>O<sub>4</sub> nanocomposites synthesized at 0 °C resulted large amount of nanorods/tubes compared with synthesized at 25 °C. It is because polymerization of nanocomposites at low temperature proceeded slowly and could form the nanorods/tubes easily compared with nanocomposites synthesized at higher temperature.

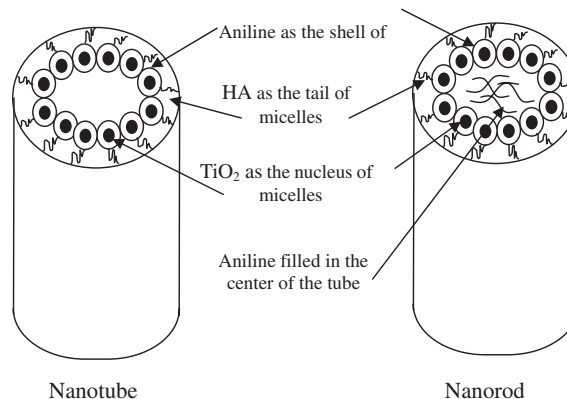


**Figure 6.** Schematic images for the resulted PANi/HA/TiO<sub>2</sub> nanorods/tubes through template free synthesis.

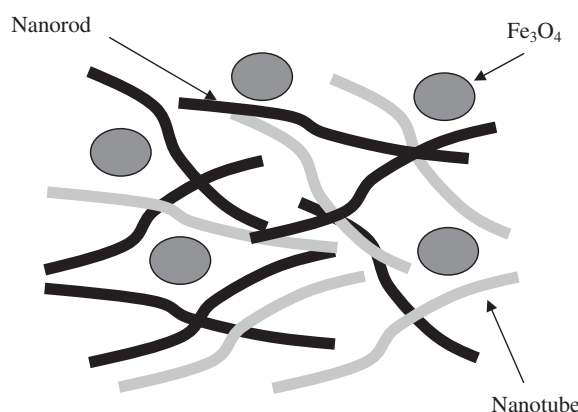


**Figure 7.** Schematic image of Fe<sub>3</sub>O<sub>4</sub> physically mixed with PANi/HA/TiO<sub>2</sub> nanorods/tubes during template free synthesis.

Refer to the SEM images in Figure 6, PANi/HA/TiO<sub>2</sub> resulted large amount of nanorods/tubes after addition of TiO<sub>2</sub> but the amount of nanorods/tubes significantly reduced after addition of Fe<sub>3</sub>O<sub>4</sub>. It is because addition of TiO<sub>2</sub> in the center of the Ani/HA micelle during template free method could activate the formation of nanorods/tubes. However, addition of Fe<sub>3</sub>O<sub>4</sub> act as the barrier that disturbed the formation of the PANi nanorods/tubes from the Ani/HA micelles and thus reduced the amount of nanorod/tubes. In this situation, some of the micelles become big sphere (such as globular or ellipsoidal shapes) by accretion instead of elongation. Based on the results that discussed above, it is reasonable to convince that the morphology (amount of nanorods/tubes) and sizes of nanostructures (diameter of nanorods/tubes) are essentially affected by the synthesis parameter such as polymerization temperature and types of filler used. This result also agreed with the results that reported by Zhang *et al.* and Wan *et al.* in which the formation of the nanostructures are significantly depend on the synthesis condition such as reaction temperature, types of filler or dopant, concentration of dopant used and so on.<sup>9,23</sup>

Electrical conductivities of PANi/HA, PANi/HA/TiO<sub>2</sub> and PANi/HA/TiO<sub>2</sub>/Fe<sub>3</sub>O<sub>4</sub> micro/nanocomposites were recorded

**Table I.** Conductivities, relative dielectric constant ( $\epsilon_r$ ) and magnetization (Saturated magnetization (Ms), remnant magnetization (Mr) and coercive force (Hc)) of PAni/HA, PAni/HA/TiO<sub>2</sub> and PAni/HA/TiO<sub>2</sub>/Fe<sub>3</sub>O<sub>4</sub> micro/nanocomposite synthesized at 0 °C and 25 °C

Sample Name	Conductivity (S/cm)	$\epsilon_r$	Ms (emu/g)	Mr (emu/g)	Hc (Oe)
PAni/HA (0 °C)	$1.0 \times 10^{-3}$	—	—	—	—
PAni/HA (25 °C)	$7.0 \times 10^{-4}$	—	—	—	—
PAni/HA/TiO <sub>2</sub> (0 °C)	$4.2 \times 10^{-4}$	-5952	—	—	—
PAni/HA/TiO <sub>2</sub> (25 °C)	$8.0 \times 10^{-4}$	2633	—	—	—
PAni/HA/TiO <sub>2</sub> /Fe <sub>3</sub> O <sub>4</sub> (0 °C)	$3.3 \times 10^{-4}$	-7381	7.7	$9.2 \times 10^{-1}$	122.7
PAni/HA/TiO <sub>2</sub> /Fe <sub>3</sub> O <sub>4</sub> (25 °C)	$4.9 \times 10^{-4}$	1234	4.7	$5.4 \times 10^{-1}$	121.6
Fe <sub>3</sub> O <sub>4</sub>	—	—	87.4	13.0	124.7

using four-probe method and the data were shown in Table I. Base on the data obtained, PAni/HA polymerized at low temperature exhibited higher conductivity ( $1.0 \times 10^{-3}$  S/cm) compared with PAni/HA polymerized at higher temperature ( $7.0 \times 10^{-4}$  S/cm). The conductivities of the PAni/HA/TiO<sub>2</sub> and PAni/HA/TiO<sub>2</sub>/Fe<sub>3</sub>O<sub>4</sub> micro/nanocomposites were relatively low ( $3.3\text{--}4.2 \times 10^{-4}$  S/cm) after addition of TiO<sub>2</sub> and Fe<sub>3</sub>O<sub>4</sub>. During this study, TiO<sub>2</sub> and Fe<sub>3</sub>O<sub>4</sub> that encapsulated in the PAni/HA matrix will partially block the PAni conductive path along the backbone of the PAni and lead to the decreasing in conductivity.

The relative dielectric constant ( $\epsilon_r$ ) (at 2.5 MHz) of PAni/HA/TiO<sub>2</sub> & PAni/HA/TiO<sub>2</sub>/Fe<sub>3</sub>O<sub>4</sub> micro/nanocomposite synthesized at 0 °C and 25 °C were recorded in Table I below. As a result,  $\epsilon_r$  of PAni/HA/TiO<sub>2</sub> & PAni/HA/TiO<sub>2</sub>/Fe<sub>3</sub>O<sub>4</sub> micro/nanocomposite synthesized 25 °C is 2633 and 1234 respectively. Generally, the dielectric constants of polymers are very low and the addition of high dielectric constant material could significantly enhance the dielectric constant of polymeric systems. Recently, it had been found that large dielectric constant could be achieved near the percolation threshold of the composite.<sup>24</sup> The micro/nanocomposites that synthesized in this study consists of three materials that possessing different conductivities and permittivities. Thus, the interface across PAni/HA with TiO<sub>2</sub> and Fe<sub>3</sub>O<sub>4</sub> may be sources that leading the large dielectric constant that posses by PAni/HA/TiO<sub>2</sub> & PAni/HA/TiO<sub>2</sub>/Fe<sub>3</sub>O<sub>4</sub> micro/nanocomposite synthesized 25 °C.<sup>16</sup> As reported by Chandrasekhar & Naishadham (1999), the high values of the dielectric constant are characteristics of conducting polymers which are partially attributed by the disordered motion of the charge carriers along the backbone of the conjugated polymer.<sup>25</sup>

On the other hand,  $\epsilon_r$  of PAni/HA/TiO<sub>2</sub> and PAni/HA/TiO<sub>2</sub>/Fe<sub>3</sub>O<sub>4</sub> micro/nanocomposite synthesized 0 °C is -5952 and -7381 respectively. The unique properties of so-called “left-handed” materials (LHM) with simultaneously negative real parts of the dielectric permittivity ( $\epsilon_r^* = \epsilon_r' - j\epsilon_r''$ ) and magnetic permeability ( $\mu_r^* = \mu_r' - j\mu_r''$ ), (including the possibility of focusing the radiation of point sources by a plane-parallel plate) were predicted by Prof. V.G. Veselago in late 1960.<sup>26</sup> After that, various options were suggested for the practical realization of several types of composites with negative values of  $\epsilon_r'$  and  $\mu_r'$ . Although the negative dielectric

constant is a new discovery in physic since year 2000 but the mechanism of this material is still not clear.<sup>27–29</sup> Negative value of dielectric constant will give rise to minimum transmission and maximum absorption that indicated good microwave absorbing property as reported by Smith *et al.* (2000).<sup>30</sup> Since the negative value of dielectric constant is a new discovery in physic since year 2000 and the mechanism of this material is still not clear, it is very difficult to explain why the negative dielectric constant is obtained at lower synthesis temperature instead of positive value.

Table I show the magnetization data on the applied magnetic field (from -10kOe to 10kOe) of Fe<sub>3</sub>O<sub>4</sub> micro-particles, PAni/HA/TiO<sub>2</sub>/Fe<sub>3</sub>O<sub>4</sub> nanocomposites synthesized at 0 °C and 25 °C. All the magnetization data recorded in Table I are saturated magnetization (Ms), remnant magnetization (Mr) and coercive force (Hc) that estimated from the magnetization curves. PAni/HA/TiO<sub>2</sub>/Fe<sub>3</sub>O<sub>4</sub> micro/nanocomposite (25 °C) under applied magnetic field at room temperature exhibited the hysteric loops (Figure 8) of the ferromagnetic behavior with the moderate saturation magnetization (Ms = 4.7 emu/g) and high coercivity (Hc = 121.6 Oe). Refer to all magnetization curves obtained, hysteresis loop appeared in Fe<sub>3</sub>O<sub>4</sub> as well as PAni/HA/TiO<sub>2</sub>/Fe<sub>3</sub>O<sub>4</sub> nanocomposites synthesized at 0 °C and 25 °C that indicated PAni/HA/TiO<sub>2</sub>/Fe<sub>3</sub>O<sub>4</sub> nanocomposites show similar ferromagnetic behavior as Fe<sub>3</sub>O<sub>4</sub> used in this study. For Fe<sub>3</sub>O<sub>4</sub> microparticles, Ms, Mr and Hc are 87.4 emu/g, 13.0 emu/g and 124.7 Oe respectively. PAni/HA/TiO<sub>2</sub>/Fe<sub>3</sub>O<sub>4</sub> nanocomposites synthesized at 0 °C exhibited higher magnetization (Ms = 7.73 emu/g) compared with nanocomposites that synthesized at 25 °C (Ms = 4.67 emu/g). As conclusion, PAni/HA/TiO<sub>2</sub>/Fe<sub>3</sub>O<sub>4</sub> nanocomposites synthesized at 0 °C shows stronger magnetic behavior compared with synthesized at 25 °C. These phenomena can be explained by the fact that Fe<sub>3</sub>O<sub>4</sub> could easily interact with PAni to form the PAni/HA/TiO<sub>2</sub>/Fe<sub>3</sub>O<sub>4</sub> micro/nanocomposites at low temperature (0 °C) compared with high temperature (25 °C) even the mass of Fe<sub>3</sub>O<sub>4</sub> adding into both samples is same (0.1 g). This fact could be proved by the TGA profile discussed before.

## CONCLUSIONS

In this communication, PAni/HA, PAni/HA/TiO<sub>2</sub> and PAni/HA/TiO<sub>2</sub>/Fe<sub>3</sub>O<sub>4</sub> were successfully synthesized through template free method under various polymerization conditions. FT/IR spectra of PAni/HA/TiO<sub>2</sub> and PAni/HA/TiO<sub>2</sub>/Fe<sub>3</sub>O<sub>4</sub> indicated the peaks are derived from HA doped PAni. The X-ray diffraction patterns of PAni/HA/TiO<sub>2</sub> and PAni/HA/TiO<sub>2</sub>/Fe<sub>3</sub>O<sub>4</sub> micro/nanocomposites clearly showed the existence of both TiO<sub>2</sub> and Fe<sub>3</sub>O<sub>4</sub>. Thermal stability of the micro/nanocomposites was being studied by TGA analysis. Nanorods/tubes shown in the SEM images indicated that PAni/HA, PAni/HA/TiO<sub>2</sub> and PAni/HA/TiO<sub>2</sub>/Fe<sub>3</sub>O<sub>4</sub> micro/nanocomposites exhibited polymerization through elongation. The diameters of PAni/HA nanorods/tubes increased from 150–180 nm to 180–200 nm (PAni/HA/TiO<sub>2</sub> and PAni/HA/TiO<sub>2</sub>/

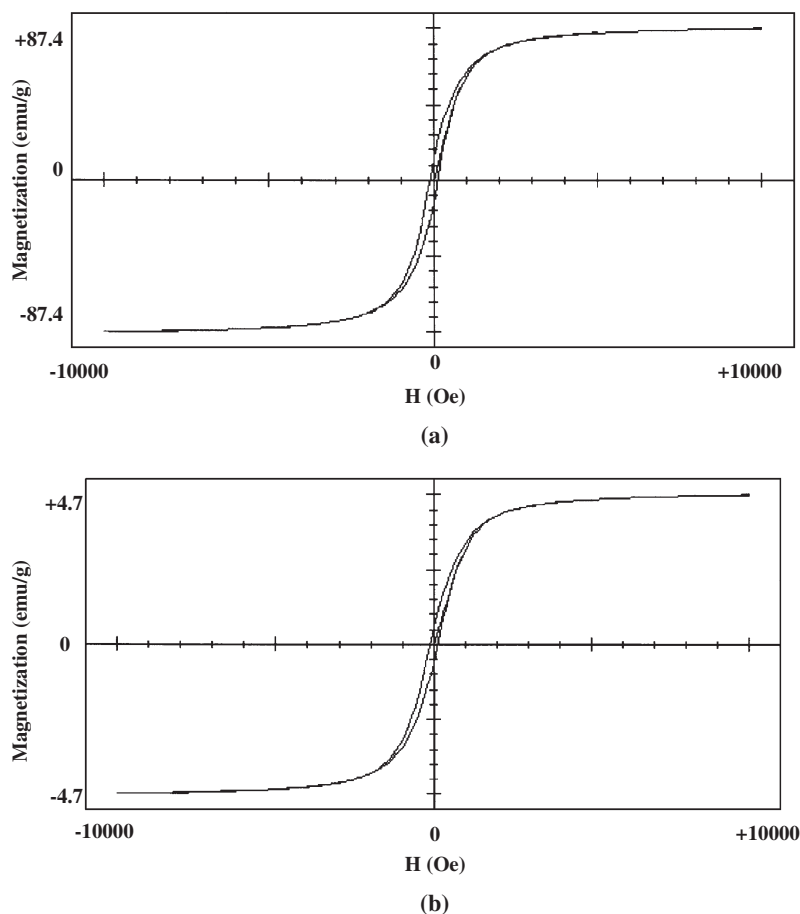


**Figure 8.** Variation of magnetization with the applied magnetic field measured at room temperature for (a)  $\text{Fe}_3\text{O}_4$  and (b) PAni/HA/TiO<sub>2</sub>/Fe<sub>3</sub>O<sub>4</sub> micro/nanocomposite synthesized at 25 °C.

Fe<sub>3</sub>O<sub>4</sub>) after addition of Fe<sub>3</sub>O<sub>4</sub> and TiO<sub>2</sub>. PAni/HA, PAni/HA/TiO<sub>2</sub> and PAni/HA/TiO<sub>2</sub>/Fe<sub>3</sub>O<sub>4</sub> micro/nanocomposites synthesized at 0 °C resulted large amount of nanorods/tubes compared with those synthesized at 25 °C. PAni/HA polymerized at low temperature exhibited higher conductivity ( $1.0 \times 10^{-3}$  S/cm) compared with PAni/HA polymerized at higher temperature ( $7.0 \times 10^{-4}$  S/cm). The conductivities of the PAni/HA/TiO<sub>2</sub> and PAni/HA/TiO<sub>2</sub>/Fe<sub>3</sub>O<sub>4</sub> micro/nanocomposites were relatively low ( $3.3\text{--}4.2 \times 10^{-4}$  S/cm) after addition of TiO<sub>2</sub> and Fe<sub>3</sub>O<sub>4</sub> due to the blocking of conductive pathways by TiO<sub>2</sub> and Fe<sub>3</sub>O<sub>4</sub> that embedded in the PAni matrix. Besides that, magnetic and dielectric behaviors of the micro/nanocomposites were measured by using vibrating sample magnetometer (VSM) and impedance analyzer respectively. As a result,  $\epsilon_r$  of PAni/HA/TiO<sub>2</sub> & PAni/HA/TiO<sub>2</sub>/Fe<sub>3</sub>O<sub>4</sub> micro/nanocomposite synthesized 25 °C is 2633 and 1234 respectively. By contrast,  $\epsilon_r$  of PAni/HA/TiO<sub>2</sub> and PAni/HA/TiO<sub>2</sub>/Fe<sub>3</sub>O<sub>4</sub> micro/nanocomposite synthesized 25 °C is -5952 and -7381 respectively. PAni/HA/TiO<sub>2</sub>/Fe<sub>3</sub>O<sub>4</sub> micro/nanocomposites synthesized at 0 °C exhibited higher magnetization ( $M_s = 7.7$  emu/g) compared with micro/nanocomposites that synthesized at 25 °C ( $M_s = 4.7$  emu/g). As conclusion, PAni/HA/TiO<sub>2</sub>/Fe<sub>3</sub>O<sub>4</sub> micro/nanocomposites that possess moderate conductivity, high dielectric

constant (or negative dielectric constant) and high magnetization that contribute to high EMI shielding efficiency (SE) and good microwave absorbing property have been successfully synthesized.

**Acknowledgment.** The author would like to show high appreciation for the Japan Government Scholarship (Monbukagakusho) for the financial support. Magnetization measurements were made at Laboratory Ishii and dielectric measurements were tested at Laboratory Hirose in Yamagata University. The authors would like to show acknowledgment to Professor Osamu Ishii and Professor Seiji Hirose for their kindly discussion and advice. Besides that, author would like to thank Mr. Masaki Nakamura for the measurement of magnetization.

Received: May 21, 2007  
Accepted: September 25, 2007  
Published: November 13, 2007

#### REFERENCES

1. A. R. Hopkins, R. A. Lipeles, and W. H. Kao, *Thin Solid Films*, **447–448**, 474 (2004).
2. B. J. Kim, S. G. Oh, M. G. Han, and S. S. Im, *Synth. Met.*, **122**, 297

- (2001).
3. M. G. Han, S. K. Cho, S. G. Oh, and S. S. Im, *Synth. Met.*, **126**, 53 (2002).
  4. S. J. Su and N. Kuramoto, *Synth. Met.*, **114**, 147 (2000).
  5. Z. Zhang and M. Wan, *Synth. Met.*, **128**, 83 (2002).
  6. Y. Duan, S. Liu, and H. Guan, *Sci. Tech. Adv. Mater.*, **6**, 513 (2005).
  7. S. K. Dhawan, N. Singh, and D. Rodrigues, *Sci. Tech. Adv. Mater.*, **4**, 105 (2003).
  8. Y. Long, Z. Chen, J. L. Duvail, Z. Zhang, and M. Wan, *Physica B*, **370**, 121 (2005).
  9. L. Zhang, L. Zhang, M. Wan, and Y. Wei, *Synth. Met.*, **156**, 454 (2006).
  10. Y. Long, Z. Chen, N. Wang, Z. Zhang, and M. Wan, *Physica B*, **325**, 208 (2003).
  11. L. Zhang, M. Wan, and Y. Wei, *Synth. Met.*, **151**, 1 (2005).
  12. M. Wan, J. Liu, H. Qiu, J. Li, and S. Li, *Synth. Met.*, **119**, 71 (2001).
  13. S. Geetha, K. K. Sathesh Kumar, and D. C. Trivedi, *Compos. Sci. Technol.*, **65**, 973 (2005).
  14. C. Y. Lee, H. G. Song, K. S. Jang, E. J. Oh, A. J. Epstein, and J. Joo, *Synth. Met.*, **102**, 1346 (1999).
  15. Z. Zhang and M. Wan, *Synth. Met.*, **132**, 205 (2003).
  16. A. Dey, S. De, A. De, and S. K. De, *Nanotechnology*, **15**, 1277 (2004).
  17. A. Chen, H. Wang, B. Zhao, and X. Li, *Synth. Met.*, **139**, 411 (2003).
  18. D. Zhong, J. J. Moore, B. M. Mishra, T. Ohno, E. A. Levashov, and J. Disam, *Surf. Coat. Technol.*, **163–164**, 50 (2003).
  19. S. H. Lu and C. W. Chung, *Mater. Lett.*, **46**, 149 (2000).
  20. Y. K. Sun, M. Ma, Y. Zhang, and N. Gu, *Colloids Surf., A*, **245**, 15 (2004).
  21. K. Shalini, G. N. Subbanna, S. Chandrasekaran, and S. A. Shivashankar, *Thin Solid Films*, **424**, 56 (2003).
  22. I. S. Lee, J. Y. Lee, J. H. Sung, and H. J. Choi, *Synth. Met.*, **152**, 173 (2005).
  23. M. Wan, Z. Wei, Z. Zhang, L. Zhang, K. Huang, and Y. Yang, *Synth. Met.*, **135–136**, 175 (2003).
  24. C. Huang, Q. M. Zhang, and J. Su, *Apply. Phys. Lett.*, **82**, 3502 (2003).
  25. P. Chandrasekhar and K. Naisdham, *Synth. Met.*, **105**, 115 (1999).
  26. V. G. Veselago, *Sov. Phys. Usp.* **10** 509 (1968).
  27. A. N. Lagarkov, V. N. Semenenko, V. A. Chistyayev, D. E. Ryabov, S. A. Tretyakov, and C. R. Simovski, *Electromagnetics*, **17**, 213 (1997).
  28. A. N. Lagarkov, V. N. Semenenko, V. N. Kisel, and V. A. Chistyayev, *J. Magn. Magn. Mater.*, **258–259**, 161 (2003).
  29. G. V. Eleftheriades, A. K. Iyer, and P. C. Kremer, *IEEE Trans. Microwave Theory Tech.* **50**, 2702 (2002).
  30. D. R. Smith, W. J. Padilla, D. C. Vier, S. C. Nemat-Nasser, and S. Schultz, *Phys. Rev. Lett.*, **84**, 4184 (2000).